ISME

An Enhanced Flux Treatment in Solving Incompressible Flow in a Forward-Facing Step

S.E. Razavi[*]
Associate Professor

S. Ezazi [†]
Lecturer

The aim of this paper is to give a detailed effect of several parameters such as step height, Reynolds number, contraction ratio, and temperature difference between the entrance and solid boundaries, of a forward-facing step. An accurate length of separation and reattachment zones are achieved. A finite-volume method (FVM) has been developed to study incompressible flow in a forward-facing step along with artificial compressibility technique. The governing equations are solved by time marching using a fifth-order Runge-Kutta time stepping. The proposed explicit finite volume method uses a new biasing discretization in space. The proposed model reveals that pressure and velocity fields are determinable in a wide range of Reynolds numbers up to 330 without artificial dissipation. The numerical results agree well with the available experimental and numerical data.

Keywords: incompressible flow, artificial compressibility, Navier-Stokes equations, finite volume, flux treatment, forward-facing step

1. Introduction

The existence of flow separation and subsequent reattachment due to a sudden compression in the flow passages, such as forward-facing steps, plays an important role in the design of a wide variety of engineering applications where heating or cooling is required. These heat transfer applications appear in cooling systems for electronic equipments, combustion chambers, and energy systems equipment, environmental control systems, high performance heat exchangers, and cooling passages in turbine blades. A great deal of mixing of high and low energy fluid occurs in the reattachment flow regions of these devices [2]. The configuration of a forward-facing step has been investigated much less than its counter part, the backward-facing step. This is mainly due to the fact that the backward-facing step is often used as a benchmark test for computations whereas the calculation of the forward-facing step is quite a delicate task. In other words, very little has been published on the problem of the laminar separation on a forward-facing step, and neither its topology nor its relevant scales are known in a predictable form. Although forward-facing step configurations appear in flows over obstacles, such as buildings [1]. In the forward-facing step, the flow field is more

[*]Corresponding Author, Associate Professor, University of Tabriz, Faculty of Mechanical Engineering
razavi@tabrizu.ac.ir
[†]Lecturer, Islamic Azad University, Ahar Branch

complicated and one or two separated regions may develop with upstream and downstream of the step [2].

An efficient code is the key to solution methodologies which would produce results using the least amount of computing time and memories. This is particularly true for problems with high Reynolds numbers. Algorithms for solving the Euler and Navier-Stokes equations with FVM have been grown in recent years [4, 5]. The FVM of Jameson et al has proved to be useful as a tool for aerodynamic applications and Navier-Stokes equations [6]. Among the various schemes proposed for the flux calculation in FVM, the Jameson's flux averaging is still of use because of its robustness. The artificial compressibility approach of Chorin [7] is applied, to incompressible Navier-Stokes equations which produces a hyperbolic dominated system of equations. It was shown by Volpe that the compressible codes can predict accurately the flow features of incompressible flows [8]. The advantage of the proposed algorithm is that it can solve the flow field at high Reynolds number up to 2300 relative to hydraulic diameter and 330 relative to step height of reference [1]. In fact we solved the two dimensional flow-field at central line and in vicinity of the step and obtained high precision numerical results and extracted the exact location of separation and exact length of recirculation region at each Reynolds number in comparison with experimental data. This problem is not well clarified by PTV method and it is not able to explain the flow quality in the vicinity of step and at the central line [1]. A pressure based method is used by Barbosa and Anand to achieve properties of flow field [3]. Wilhelm and Kleiser presented some results using spectral element method. The present benchmark case suffers from the lack of published works in the technical literature. Therefore, the authors have tried to give the maximum possible effort in this regard. In this work the finite-volume method is equipped by a biased flux treatment to simulate the flow behavior in a forward-facing step. A set of upwind-biased schemes, has recently been cited in [9]. Also, a class of characteristic based schemes has been developed based on wave propagation, applying to backward-facing step [10].

2. Governing Equations

The integral form of Navier-Stokes equations with artificial compressibility can be written as:

$$\frac{\partial}{\partial t}\iint_{A} U d\Omega + \oint_{\partial A}(F dy - G dx) = \oint_{\partial A}(R dy - S dx) \tag{1}$$

$$U = \begin{bmatrix} p \\ u \\ v \\ \theta \end{bmatrix}, \quad F = \begin{bmatrix} \beta u \\ u^2 + p \\ uv \\ u\theta \end{bmatrix}, \quad G = \begin{bmatrix} \beta v \\ uv \\ v^2 + p \\ v\theta \end{bmatrix}, \quad R = \frac{1}{Re}\begin{bmatrix} 0 \\ \frac{\partial u}{\partial x} \\ \frac{\partial v}{\partial x} \\ \frac{1}{Pr}\frac{\partial \theta}{\partial x} \end{bmatrix}, \quad S = \frac{1}{Re}\begin{bmatrix} 0 \\ \frac{\partial u}{\partial y} \\ \frac{\partial v}{\partial y} \\ \frac{1}{Pr}\frac{\partial \theta}{\partial y} \end{bmatrix} \tag{2}$$

in which A and ∂A are the domain area and perimeter respectively. The β is artificial compressibility parameter and Re is based on the step height. Pr shows the Prandtl number assumed to be constant. Equation (1) is in non-dimensional form by applying the following relations:

$$x^* = \frac{x}{h},\ y^* = \frac{y}{h},\ u^* = \frac{u}{V_0},\ v^* = \frac{v}{V_0} \tag{3}$$
$$p^* = \frac{p - p_0}{\rho_0 V_0^2},\ \theta^* = \frac{T - T_0}{T_w - T_0},\ t^* = \frac{tV_0}{h},\ Pr = \frac{\upsilon}{\alpha}$$

Where θ^* denotes the uniform wall temperature. For simplicity the * has been eliminated in equation (1). The grid is generated algebraically and shown in figure 1.

3. Discretization of the Governing Equations

3.1. Space Discretization

The second term of equation (1) is discretized over the face as in figure 2:

$$\oint_{ABCD} (Fdy - Gdx) = \sum_{k=1}^{4} (F_k \Delta y_k - G_k \Delta x_k) \tag{4}$$

As an example:

$$F_1 = \frac{F_{i,j} + F_{i+1,j}}{2} \tag{5}$$

The enhanced flux treatment plays an important role in accuracy and stability of solutions. A pressure based flux upwinding has been used by defining a parameter as:

$$\xi = \frac{p_{i,j}}{p_{i,j} + p_{i+1,j}} \tag{6}$$

For example, at right side of primary cell, flux averaging is computed by $F_{AB} = \xi F_{i,j} + (1-\xi)F_{i+1,j}$ or $F_1 = \xi F_{i,j} + (1-\xi)F_{i+1,j}$ instead of relation (5).
The second-order derivatives are discretized as the following manner:

$$\oint (Rdy - Sdx) = \oint \left(\left[\frac{\partial \phi}{\partial x}\right] dy - \left[\frac{\partial \phi}{\partial y}\right] dx \right) \tag{7}$$
$$\approx \sum_{k=1}^{4} \left(\left[\frac{\partial \phi}{\partial x}\right]_k \Delta y_k - \left[\frac{\partial \phi}{\partial y}\right]_k \Delta x_k \right)$$

ϕ stands for u, v, θ. Applying relation (7) on cell ABCD yields:

$$\begin{aligned}\oint(\mathrm{Rdy}-\mathrm{Sdx}) &= \left[\frac{\partial\phi}{\partial x}\right]_{AB}\Delta y_{AB}-\left[\frac{\partial\phi}{\partial y}\right]_{AB}\Delta x_{AB}\\ &+\left[\frac{\partial\phi}{\partial x}\right]_{BC}\Delta y_{BC}-\left[\frac{\partial\phi}{\partial y}\right]_{BC}\Delta x_{BC}\\ &+\left[\frac{\partial\phi}{\partial x}\right]_{CD}\Delta y_{CD}-\left[\frac{\partial\phi}{\partial y}\right]_{CD}\Delta x_{CD}\\ &+\left[\frac{\partial\phi}{\partial x}\right]_{DA}\Delta y_{DA}-\left[\frac{\partial\phi}{\partial y}\right]_{DA}\Delta x_{DA}\end{aligned} \tag{8}$$

For calculating $\frac{\partial\phi}{\partial y}$ and $\frac{\partial\phi}{\partial x}$ the secondary cells are used. As an instance at face AB from AEBM secondary cell, one has:

$$\left[\frac{\partial\phi}{\partial x}\right]_{AB}=\frac{1}{s'}\iint_{s'}\frac{\partial\phi}{\partial x}ds=\frac{1}{s'}\oint_{\partial s'}\phi dy=\frac{1}{s'}\sum_{k=1}^{4}\phi_k\Delta y_k \tag{9}$$

$s'=s_{AEBM}$

$$\begin{aligned}\left[\frac{\partial\phi}{\partial x}\right]_{AB} &= \frac{1}{s'}[0.5(\phi_E+\phi_A)\Delta y_{AE}+0.5(\phi_E+\phi_B)\Delta y_{EB}\\ &+0.5(\phi_B+\phi_M)\Delta y_{BM}+0.5(\phi_M+\phi_A)\Delta y_{MA}]\end{aligned} \tag{10}$$

$$\begin{aligned}\left[\frac{\partial\phi}{\partial y}\right]_{AB} &= -\frac{1}{s'}[0.5(\phi_E+\phi_A)\Delta x_{AE}+0.5(\phi_E+\phi_B)\Delta x_{EB}\\ &+0.5(\phi_B+\phi_M)\Delta x_{BM}+0.5(\phi_M+\phi_A)\Delta x_{MA}]\end{aligned} \tag{11}$$

For example:

$$\Delta y_{EB}=y_B-y_{E,}\quad \Delta x_{EB}=x_B-x_E \tag{12}$$

$$\phi_A=\frac{1}{4}(\phi_{SE}+\phi_S+\phi_M+\phi_E) \tag{13}$$

$$\mathrm{vol.}\frac{\partial U}{\partial t}+\sum_{k=1}^{4}(F_k\Delta y_k-G_k\Delta x_k)=\sum_{k=1}^{4}(R_k\Delta y_k-S_k\Delta x_k) \tag{14}$$

3.2. Time Discretization

A fifth-order Runge-Kutta algorithm is used for time discretization because of its wide range of stability and rapid convergence in comparison to other schemes. By averaging the flow parameters over a cell equation (1) becomes:

$$\frac{\partial\overline{U}}{\partial t}=\frac{1}{S''_{ABCD}}\left[\oint(\mathrm{Rdy}-\mathrm{Sdx})-\oint(\mathrm{Fdy}-\mathrm{Gdx})\right] \tag{15}$$

Where as $\overline{U}$ is mean value of variables over the cell and S'' is the cell area.

The equation (15) is considered as follow:

$$\frac{\partial \overline{U}}{\partial t} + Q(U) = 0 \tag{16}$$

In which a fifth-order Runge-Kutta algorithm is applied as:

$$U^m = U^0 - \alpha_m \Delta t Q^{(m-1)}(U), \quad \alpha_m = 1/4,\ 1/6,\ 3/8,\ 1/2,\ 1 \quad m = 1,2,3,4,5 \tag{17}$$

4. Boundary conditions

Consistent solid boundary conditions must ensure the disturbance dissipation in the discretized domain without reflection. On the solid boundaries, the usual no-slip conditions is applied, i.e. $u = 0,\ v = 0$. For the temperature and pressure, $\theta = 1,\ p_{si} = 1.5p_{i,1} - 0.5p_{i,2}$ where p_{si} implies the solid boundary pressure. The inflow boundary conditions are computed by $v = 0,\ p = 1.5p_{i,j} - 0.5p_{i+1,j},\ T = T_0$.

To provide a fully developed velocity profile a parabolic profile at inlet is used i.e. $u = (-3y^2 + 12y)/8$ this profile satisfies corresponding boundary conditions. For outflow boundary conditions (u, v, T) are extrapolated from inside of computational domain while the pressure is fixed.

5. Numerical results and discussion

To investigate the performance of the proposed FVM, a series of tested were conducted. Error norm is defined by:

$$\text{Error} = \frac{\sum_{i=1}^{N}\sum_{j=1}^{M}\sqrt{(u_{i.j}^{n+1} - u_{i,j}^{n})^2}}{N \times M} \le 10^{-8} \tag{18}$$

where *N* and *M* are the cell numbers in horizontal and vertical directions respectively. In this research a complete study for possible cases that can exist in engineering problems is done. Grid independencies have accomplished for Reynolds number 330 in figure 3 by four levels of grids namely $40 \times 240,\ 40 \times 360,\ 60 \times 240$ and 60×360. In fact, the difference in velocity profile appeared to be negligible for four finest successive levels of grids. This has leaded us to use mentioned grids in all subsequent calculations considering relative cost of computation with achievable accuracy. In order to study the effect of artificial compressibility parameter on the solution accuracy, the distribution of local Nusselt number for different values of it are plotted at Re=200 in figure 4. This figure 4 reveals that the steady-state results are not sensitive to artificial compressibility parameter, although our findings illustrated that its value influences stability and convergence rate of the solution. For this particular case study, artificial compressibility method parameter of 1 shows better behavior. In figure 5, the enhanced method resulted in a faster convergence rate. Figure 6 shows substantial agreement between Nusselt number by this research and other numerical results. At the channel entrance the distribution of Nusselt number starts with a high value and behaves as the classical thermal entry flow problem. However, at the vicinity of the step edge the Nusselt distribution

suddenly decreases. This particular behavior is associated with the recirculation zone upstream of the step and adjacent to the bottom wall. Then it is observed that the distribution sudden increases to a maximum value due to the cause of the sudden contraction.

The numerical results agree well with the available experimental and numerical data. Figures 7, 8, 9 and 10 represents stream lines and separation location for the selected Reynolds numbers to show different cases for creation diverse recirculation regions up stream and together upstream and down stream of step. It is observed that as contraction ratio (H/h) increases, down stream recirculation region disappears and also, as Reynolds number increases the presence of recirculation regions become more prominent by having larger regions of negative u-velocity component in the x, y coordinate directions. Streamline plots show that recirculation region place and its length is a direct function of boundary layer thickness approaching the step and step height (δ / h). Same results are present for lower Re numbers (165, 134, 50, 10).

6 . Conclusion

In present research, a FVM second order scheme is developed to solve incompressible flows. Convective flux terms are discretized first turn by averaging and second turn by enhanced flux treatment which results in more rapid convergence rate. Viscous and thermal conduction terms are discretized by a second-order technique. Governing equations are discretized in time by fifth-order Runge-Kutta scheme. Artificial compressibility technique is employed to couple continuity to momentum equation.

References

[1] Stuer, H., Gyr, A., and Kinzelbach, W., “Laminar Separation on a Forward-facing Step”, European Journal of Mechanics B/Fluids, Elsevier, Paris, Vol. 18, pp. 675-692, (1999).

[2] Abu-Mulaweh, H. I., “A Review of Research on Laminar Mixed Convection Flow Over Backward and Forward-facing Steps”, International Journal of Thermal Sciences, Elsevier, Vol. 42, pp. 897-909, (2003).

[3] Barbosa, J. G., and Anand, N. K., “Flow Over a Three-dimensional Horizontal Forward-facing Step”, Numerical Heat Transfer, Part A, Vol. 53, pp. 1-17, (2008).

[4] Jameson, A., Schmidt, W., and Turkel, E., “Numerical Solutions of the Euler Equations by Finite Volume Methods using Runge-Kutta Time-stepping Schemes”, AIAA 14th Fluid and Plasma Dynamics Conference, Palo Alto, (1981).

[5] Razavi, S. E., Mirzaee, B., and Khoshravan, E., “Finite-volume Solution of a Circular Cylinder in Cross Flow with Heat Transfer”, IJE Transactions A: Basics, Vol. 15, No. 3, pp. 303-314, (2002).

[6] Pan, D., and Cheng, J. C., “Upwind Finite-volume Navier-Stokes Computation on Unstructured Triangular Meshes”, AIAA Journal, Vol. 31, No. 9, (1993).

[7] Chorin, A. J., “A Numerical Method for Solving Incompressible Viscous Flow Problems”, Journal of Computational Physics, Vol. 2, No. 1, pp. 12-26, (1967).

[8] Volpe, G., "On the use and Accuracy of Compressible Flow Codes at Low Mach Numbers", AIAA 91-1662, (1991).

[9] Blazek, J., "*Computational Fluid Dynamics: Principles and Applications*", Elsevier, pp. 440, (2001).

[10] Zamzamian, K., and Razavi, S. E., "Multidimensional Upwinding for Incompressible Flow Based on Characteristics", Journal of Computational Physics, Vol. 228, pp. 8699-8713, (2008).

Nomenclature

$A, \partial A$: Domain area and perimeter
CFL: Courant-Friedrichs-Levy number
F, G: Convective flux vectors
H/h: Contraction ratio
M: Center of cell
M, N: Cell numbers
Nu: Nusselt number
p: Pressure
Pr: Prandtl number
R, S: Viscous flux vectors
Re: Reynolds number
S'' : Cell area
s' : Secondary cell area
T: Temperature
t: Dimensionless time
U: Dimensionless state vector
u : Horizontal dimensionless velocity component
V_0 : Free stream velocity
v : Vertical dimensionless velocity component
x, y: Physical coordinates

Greek symbols

α : Runge-Kutta coefficient
β : Artificial compressibility parameter
δ : Boundary layer thickness
ϕ : Stands for u, v, θ
θ : Dimensionless temperature
υ : Kinematic viscosity
ξ : Enhanced flux treatment parameter

Subscripts and superscripts

w: Wall

0 : Environment

* : Dimensionless

_: Mean

Figures

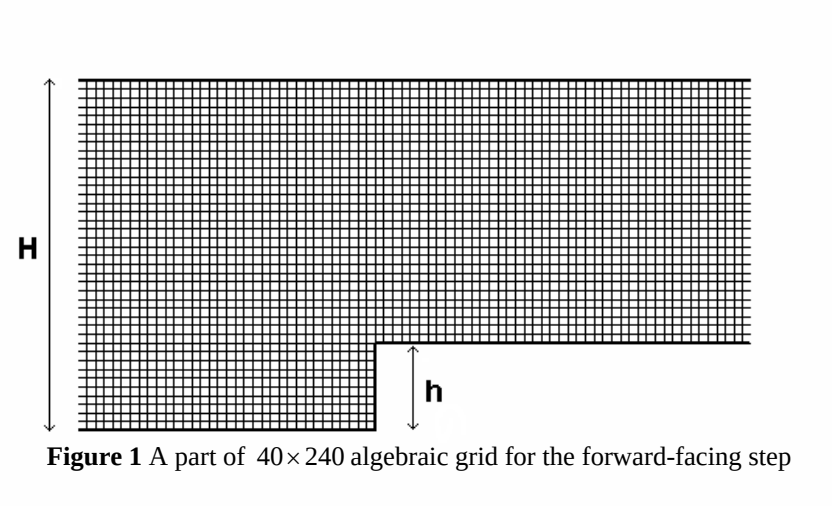

Figure 1 A part of 40×240 algebraic grid for the forward-facing step

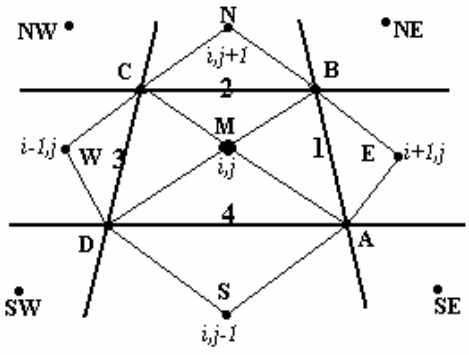

Figure 2 Primary cells (bold lines) and secondary cells (thin lines) in the finite-volume method

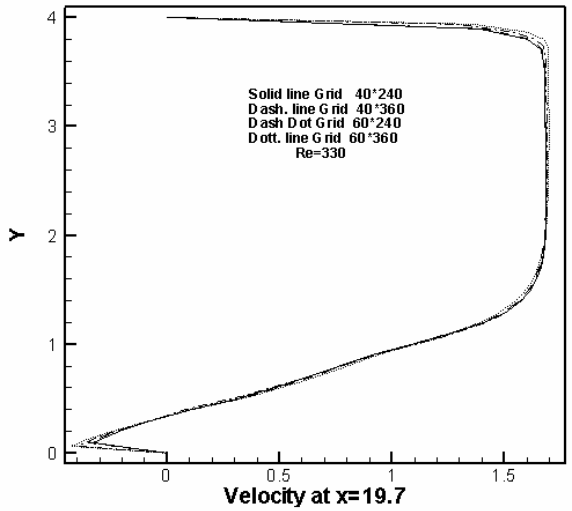

Figure 3 Grid independency

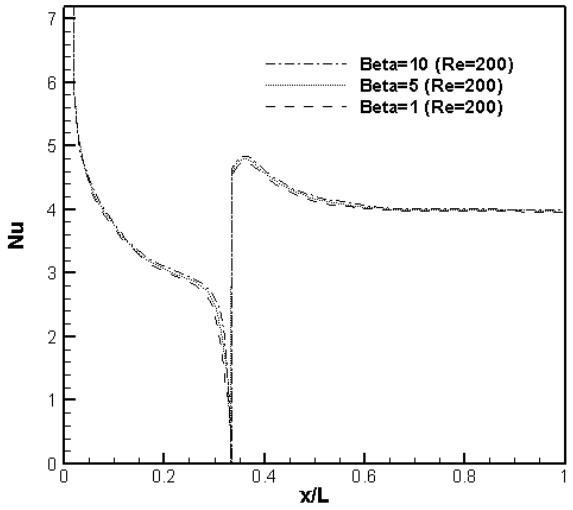

Figure 4 Independency of results to the artificial

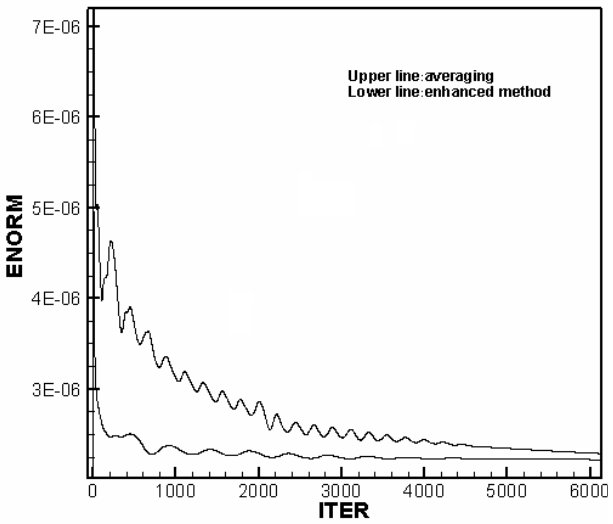

Figure 5 Comparison of convergence rates between averaging and enhanced method for Re=134

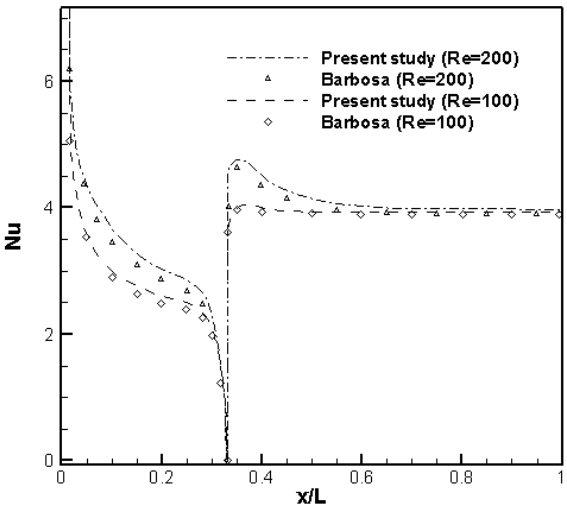

Figure 6 Comparison of Nusselt number

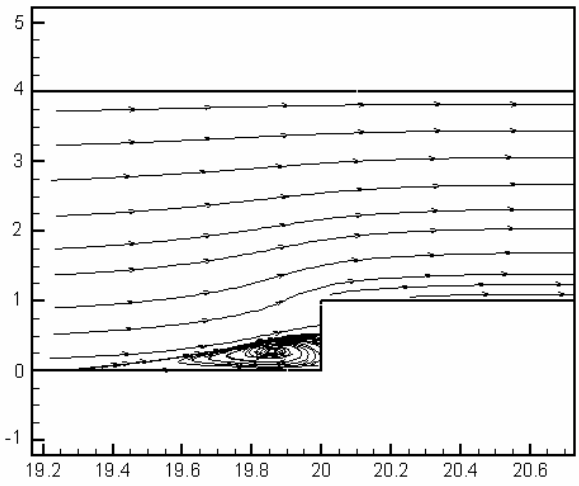

Figure 7 Streamlines for Re=330 with contraction ratio (H/h)=4

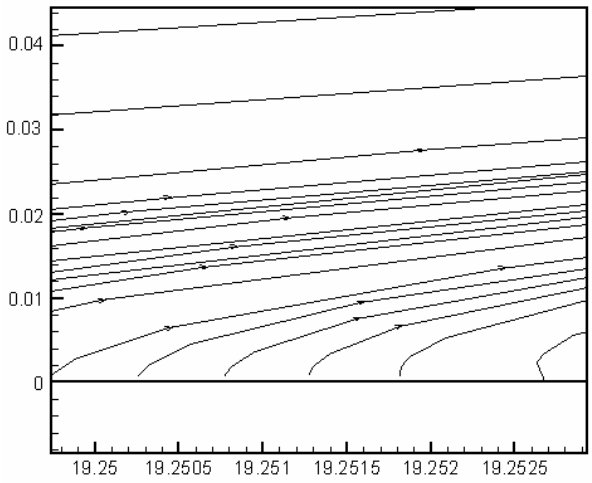

Figure 8 Separation location for Re=330 contraction ratio (H/h)=4

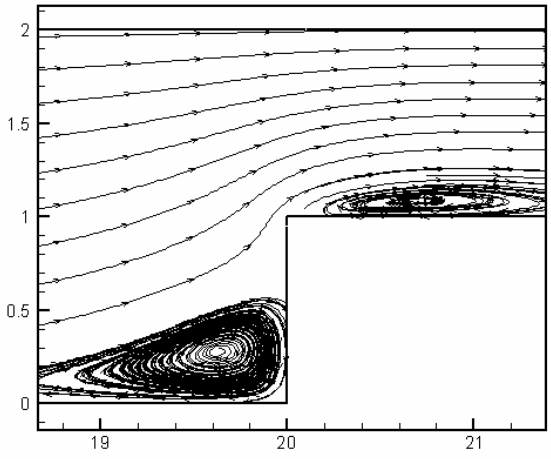

Figure 9 Streamlines for Re=330 with contraction ratio (H/h)=2

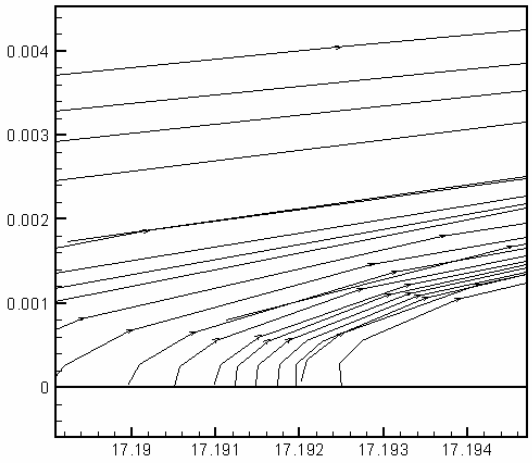

Figure 10 Separation location for Re=330 contraction ratio (H/h)=2

چکیده

هدف این مقاله ارائه تاثیر چند پارامتر مانند ارتفاع پله، عدد رینولدز، نسبت انقباض و اختلاف دما بین مقطع ورودی جریان و مرزهای جامد در هندسه پله رو به جلو می باشد. طول دقیق نواحی جدایش جریان و پیوست دوباره آن ارائه شده است. روشی حجم محدود با به کارگیری تکنیک تراکم پذیری مصنوعی برای مطالعه جریان تراکم ناپذیر در هندسه پله رو به جلو توسعه داده شده است. معادلات حاکم بر رفتار جریان سیال با استفاده از الگوی زمانروی رانگ- کوتای مرتبه پنج حل شده اند. مدل پیشنهادی، میدانهای فشار و سرعت را که در گستره وسیعی از اعداد رینولدز تا ۳۳۰ بدون اتلاف عددی مصنوعی قابل تعیین اند، آشکار می کند. نتایج عددی با داده های تجربی و عددی موجود، تطابق خوبی دارند.